AGU PUBLICATIONS

Geophysical Research Letters

RESEARCH LETTER
10.1002/2016GL069479

Key Points:
- Antarctic shelf circulation and exchange is investigated with a unique Antarctic polynya data set
- Surface flux seasonality drives circulation, influencing AABW formation and ice-ocean interactions
- Winter buoyancy losses form dense shelf water, driving circulation and enhanced cross-shelf exchange

Supporting Information:
- Supporting Information S1

Correspondence to:
K. Snow,
kate.snow@anu.edu.au

Citation:
Snow, K., B. M. Sloyan, S. R. Rintoul, A. McC. Hogg, and S. M. Downes (2016), Controls on circulation, cross-shelf exchange, and dense water formation in an Antarctic polynya, *Geophys. Res. Lett.*, *43*, 7089–7096, doi:10.1002/2016GL069479.

Received 6 MAY 2016
Accepted 13 JUN 2016
Accepted article online 15 JUN 2016
Published online 8 JUL 2016

Controls on circulation, cross-shelf exchange, and dense water formation in an Antarctic polynya

K. Snow[1], B. M. Sloyan[2], S. R. Rintoul[2,3,4], A. McC. Hogg[1], and S. M. Downes[3]

[1] ARC Centre of Excellence for Climate System Science and Research School of Earth Sciences, Australian National University, Canberra, ACT, Australia, [2] Oceans and Atmosphere, CSIRO, Hobart, Tasmania, Australia, [3] Antarctic Climate and Ecosystems Cooperative Research Centre, University of Tasmania, Hobart, Tasmania, Australia, [4] Centre for Australian Weather and Climate Research, Hobart, Tasmania, Australia

Abstract Circulation on the Antarctic continental shelf influences cross-shelf exchange, Antarctic Bottom Water formation, and ocean heat flux to floating ice shelves. The physical processes driving the shelf circulation and its seasonal and interannual variability remain poorly understood. We use a unique time series of repeat hydrographic observations from the Adélie Land continental shelf and a box inverse model to explore the relationship between surface forcing, shelf circulation, cross-shelf exchange, and dense water formation. A wind-driven northwestward coastal current, set up by onshore Ekman transport, dominates the summer circulation. During winter, strong buoyancy loss creates dense shelf water. This dense water flows off the shelf, with a compensating on-shelf flow that is an order of magnitude larger in winter than in summer. The results demonstrate the importance of winter buoyancy loss in driving the shelf circulation and cross-shelf exchange, as well as dense water mass formation.

1. Introduction

Circulation and the cross-shelf exchange of water masses on the Antarctic continental shelf influence ice shelf basal melting and the export of Antarctic Bottom Water (AABW). AABW forms an important component of the meridional overturning circulation; it sets the deep ocean stratification and transports heat, carbon, and nutrients throughout the globe [*Johnson*, 2008; *Kuhlbrodt et al.*, 2007; *Ríos et al.*, 2012; *Purkey and Johnson*, 2013]. Dense Shelf Water (DSW), the precursor to AABW, is formed by strong buoyancy loss in coastal polynyas resulting from cooling and brine rejection released by the freezing of sea ice. However, the processes regulating the formation of AABW and resulting cross-shelf exchange remain poorly understood.

The Adélie region, East Antarctica, and the Mertz polynya (located above the Adélie Depression; Figure 1) is a significant source of AABW [*Rintoul*, 1998; *Kusahara et al.*, 2010; *Williams et al.*, 2010; *Lacarra et al.*, 2011]. Polynya activity and seasonality of buoyancy fluxes potentially influence the seasonal cross-shelf exchange [*Snow et al.*, 2016], circulation, and in turn, AABW formation. By assessing the seasonality of the Adélie Land shelf circulation and the role of buoyancy fluxes within the Mertz polynya (recorded as the third largest sea ice producer of all Antarctic polynyas [*Tamura et al.*, 2008]), we provide insight into the role of surface forcing in driving the formation of DSW and exchange of water masses across the Antarctic continental shelf break. Additionally, calving of the Mertz Glacier Tongue (MGT; Figure 1) in February 2010 significantly altered the surface forcing in the region, reducing sea ice production by up to 40% [*Tamura et al.*, 2012; *Nihashi and Ohshima*, 2015]. Little is known about how such changes influenced the shelf circulation and, in turn, the water mass transport beneath ice shelves [e.g., see *Hellmer et al.*, 2012] and subsequent feedbacks on the freshwater budget [*Kusahara et al.*, 2011b; *Lacarra et al.*, 2014].

Here we exploit a time series of repeat hydrography to explore the response of this bottom water formation region to seasonal and interannual variations in surface forcing. The availability of observations spanning a range of forcing conditions (winter and summer, precalving and postcalving) makes the Adélie Land coast a particularly useful case study for investigating the sensitivity of shelf circulation and water mass formation to changes in surface forcing.

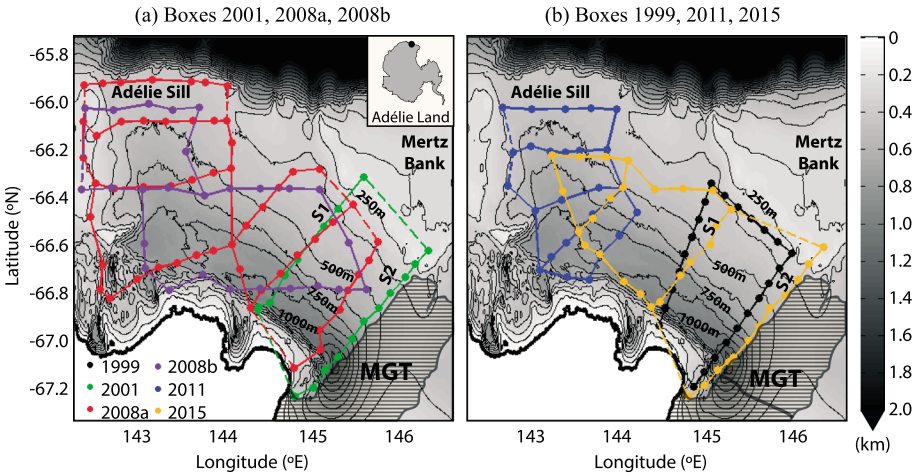

Figure 1. CTD locations and boxes for voyages (a) 2001 (green), 2008a (red), and 2008b (purple) and (b) 1999 (black), 2011 (blue), and 2015 (orange). Dashed lines indicate open borders with assumed near-zero transport. Contours show bathymetry at 125 m intervals and the hatched region represents the Mertz Glacier Tongue (MGT) before and after the calving.

2. Method

2.1. Hydrographic Data

A total of six conductivity-temperature-depth (CTD) data sets are used to derive the Adélie region circulation, including a single winter realization (1999) and five summer data sets (three prior to the MGT calving and two postcalving; Table 1 and Figure 1). All CTD measurements are calibrated with in situ bottle salinity samples, except 2008a [*Lacarra et al.*, 2011], which was calibrated before and after the voyage to remove drift. The calibrated CTD data are processed to 1–2 dbar bins.

The three occupations of the box defined by sections S1 and S2 made in 1999 are averaged to a single box. The two sets of measurements along S2 in 2001 are similarly averaged. Prior to implementing the box model, temperature and salinity are smoothed horizontally and vertically. Smoothing removes high-frequency variability, providing a more robust representation of the regional circulation. A weighted least squares smoothing is applied in the horizontal (span width of five data points weighted by station separation and decreasing to 0 weighting at outer points), while a moving average filter of width 20 dbar is implemented in the vertical.

2.2. The Inverse Box Model

Inverse box models implement conservation constraints within closed volumes defined by hydrographic sections and land boundaries [*Wunsch*, 1978]. The flow is assumed to be in hydrostatic and geostrophic balance. Geostrophic velocity relative to a reference level, v_r, is calculated from horizontal density gradients using the thermal wind balance [*McDougall and Barker*, 2011]. The initial reference velocity ($v_b = 0$ m s^{-1} at the deepest common depth of each station pair) is adjusted to conserve mass, heat, and salt, adding to v_r to give the total velocity. To account for water mass transformation within coastal polynyas we incorporate diapycnal fluxes between layers [*Sloyan and Rintoul*, 2000, 2001a, 2001b].

Table 1. Summary of CTD Cruise Information Including Cruise Date, Name, Ship, and References

Name	Cruise	Date	Ship	Reference
1999	AU9901	29/7/1999 to 23/8/1999	*Aurora Australis*	*Rosenberg et al.* [2001]
2001	NBP00-08	20/12/2000 to 25/1/2001	*Nathaniel B Palmer*	*Jacobs* [2004]
2008a	AU0803	22/12/2007 to 19/1/2008	*Aurora Australis*	*Rosenberg and Rintoul* [2010]
2008b	ALBION-2008	10/1/2008 to 19/1/2008	*Astrolabe*	*Lacarra et al.* [2011]
2011	AU1121	4/1/2011 to 06/2/2011	*Aurora Australis*	*Rosenberg and Rintoul* [2011]
2015	AU1402	5/12/2014 to 25/1/2015	*Aurora Australis*	*Rosenberg and Rintoul* [2015]

The volumes over which the inverse model is applied are shown in Figure 1 (dashed sections are treated as closed walls). The inverse model conserves quantities over the whole volume, as well as within isopycnal layers. Layers corresponding to the major water masses are defined by potential density surfaces: Antarctic Surface Waters (AASW; $\sigma_0 < 27.75$ kg m^{-3}), Modified Circumpolar Deep Water* (MCDW*; $27.75 \leq \sigma_0 < 27.88$ kg m^{-3}), and Dense Shelf Waters (DSW; $\sigma_0 \geq 27.88$ kg m^{-3}), with each water mass separated into intermediate layers (total 27–34). Note, MCDW* includes water masses of varying temperature and salinity, including the traditional warm salty MCDW (temperatures between $1 > \theta > -1.75$°C), and the cooler fresher waters ($\theta \leq -1.75$°C) found on the shelf. Additionally, we define Ice Shelf Water (ISW) as waters colder than the 50 dbar freezing temperature [*Cougnon et al.*, 2013].

With more unknown variables than model equations, the model is underdetermined. A solution is found by minimizing a quadratic cost function incorporating a priori estimates of the solution and equation errors [*Wunsch*, 1996; *Sloyan and Schröter*, 2001]. Details of the a priori error specification and the sensitivity of the solution to these errors are provided in the supporting information.

Transport error estimates are the formal errors of the inverse model, i.e., the sum of the null space errors and noise [*Wunsch*, 1978]. These errors reflect how well constrained the inverse model is. Limited winter hydrographic sections and uncertainty in the prescribed buoyancy fluxes mean that winter circulation errors are larger than those in summer. The formal errors are expected to be smaller than the uncertainty arising from temporal and spatial circulation variability. In addition to the formal model errors, the residuals of the volume conservation constraints provide a lower bound on the uncertainty.

2.3. Surface Buoyancy Fluxes

To account for the influence of winter buoyancy forcing on water mass transformation, circulation, and cross-shelf exchange, surface forcing is included in the inverse model conservation equations. We use observations taken during the 1999 winter cruise to estimate heat and salt fluxes. Sea ice production is set to 4 cm d^{-1} [*Lytle et al.*, 2001].

We apply a heat flux of 205 ± 50 W m^{-2} in the box bounded by S1 and S2. *Roberts et al.* [2001] find higher values (249–574 W m^{-2}) in the most active region of the polynya near the coast, but their values are not likely typical for the Adélie shelf. The heat flux we impose is similar to estimates of heat loss from the Mertz polynya of 204 W m^{-2} [*Williams and Bindoff*, 2003] and 175–200 W m^{-2} [*Marsland et al.*, 2004], and 249 W m^{-2} during calm conditions near the coast [*Roberts et al.*, 2001].

During summer, surface buoyancy losses are minimal while warming, precipitation and ice melt may lead to buoyancy gain. Such gains occur at the surface layer and do not influence layer-to-layer mass transfer; we thus assume heat and salt conservation with no surface heat/salt fluxes in summer.

3. Results

The circulation on the Adélie shelf is distinctly different in summer and winter (Figure 2). During winter, a cyclonic flow carries 0.46 ± 0.02 Sv (sverdrup; 10^6 m^3/s) of DSW northwest along the depression toward the Adélie Sill and 0.50 ± 0.01 Sv of MCDW* southeastward from the north (Figure 2a). A significant portion (0.29 ± 0.03 Sv; 62%) of the northwestward flowing DSW is formed through water mass transformation of lighter AASW/MCDW* to denser DSW (diapycnal fluxes; Figure 2a inset; where positive fluxes illustrate formation). A small portion of DSW (0.05 ± 0.01 Sv) also flows southeastward from the depression (Figure 2a), toward the MGT [*Williams and Bindoff*, 2003; *Cougnon et al.*, 2013]. Residual volume transport of DSW and MCDW* accounts for 0.16 Sv error in the calculated total flux.

In winter, the southeastward flow of MCDW* across S1 is dominated by cooler water classes (Figure 2a, orange), while water as warm as −1.0°C is expected at the shelf break [*Williams and Bindoff*, 2003]. We argue that on-shelf flowing waters are cooled by surface buoyancy loss and the resultant convection, leading to temperatures < −1.5°C within the S1 MCDW* layer.

The summer circulation is dominated by a shelf-wide northwestward coastal current, originating east of the MGT and likely continuing westward along the shelf break (note, the method only resolves the component of the flow perpendicular to the sections). Only in the northern areas, near the Mertz Bank and on the eastern side of the Adélie Sill, is a weak southeastward on-shelf flow of MCDW* and AASW evident. Coastal current

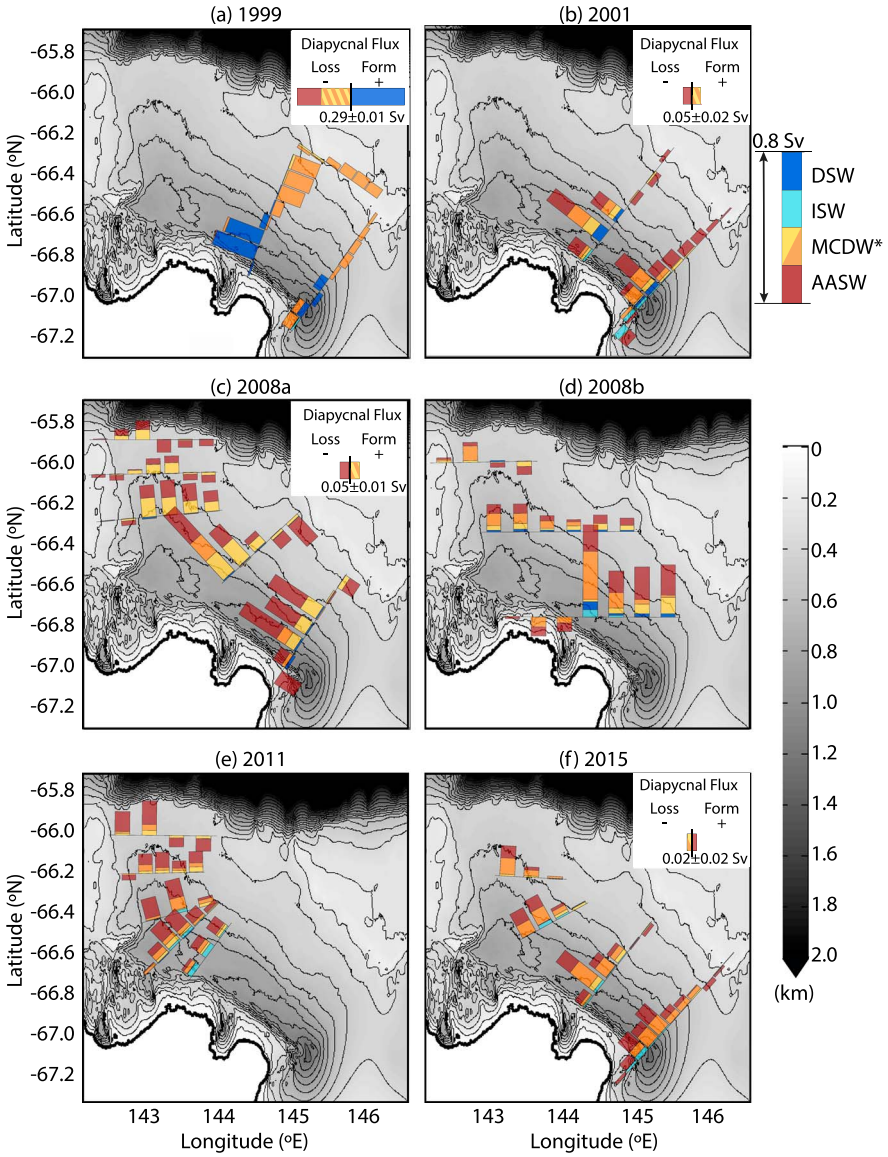

Figure 2. Net mass flux transport at station pairs for the (a) 1999 winter and (b) 2001, (c) 2008a, (d) 2008b, (e) 2011, and (f) 2015 summers, separated into density classes of Dense Shelf Water (DSW; dark blue), Ice Shelf Water (ISW; light blue), Modified Circumpolar Deep Water* (MCDW*; yellow/orange), and Antarctic Surface Waters (AASW; red). MCDW* includes warm salty (θ of 1 to −1.75°C; yellow) and cold and fresh (orange) water masses. Diapycnal fluxes are those over the polynya region (boxes containing S1 and S2; Figure 1). Positive diapycnal fluxes represent water mass formation and vice versa. Contours show bathymetry at 125 m intervals. The 2008a and 2008b differences are possibly a result of different CTD calibrations (section 2.1). Note that not all sections are shown to maintain clarity.

strength varies between years, with net northwestward fluxes through S1 and S2 being 0.72 ± 0.04 Sv in 2001, 0.91 ± 0.03 Sv in 2008a, and 0.62 ± 0.03 Sv in 2015. The 2015 northwestward transport is weaker than that observed in 2001 and 2008a, but the change in the circulation postcalving is small relative to transport variability prior to calving. Most of the summer coastal current is AASW (38–59% through S1) or MCDW* (37–50% through S1), with residuals of 0.04 Sv in 2001, 0.01 Sv in 2008a, and 0.05 Sv in 2015 in the box bounded by S1 and S2.

The warm salty water masses within the MCDW* density class (yellow in Figure 2) are most evident in the northeastern areas, while the coastal current is strongest on the southwestern side of the shelf. DSW, while widespread prior to the MGT calving, is no longer present in the 2011 and 2015 sections. Diapycnal mass fluxes

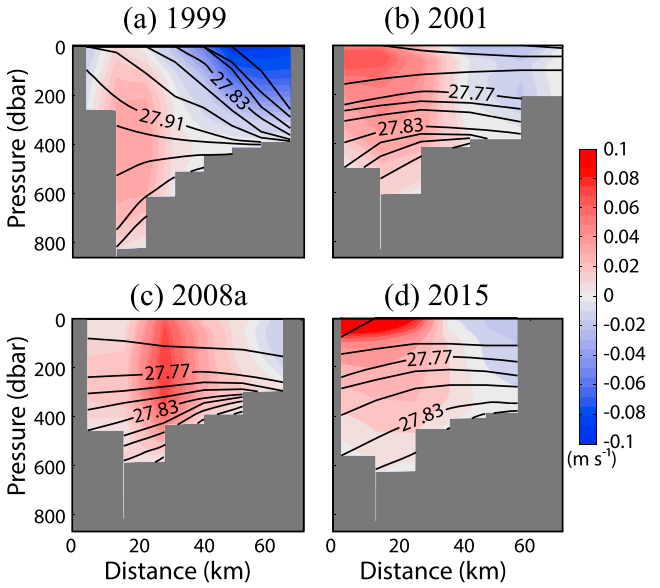

Figure 3. Velocity (m s^{-1}) through section S1 (Figure 1) for the (a) 1999 winter and (b) 2001, (c) 2008a, and (d) 2015 summers, where positive is northwestward. Contours show density (σ_0; kg m^{-3}) levels going from 26.75 to 27.91 at 0.02 kg m^{-3} intervals, and from 27.91 to 27.95 at 0.01 kg m^{-3} intervals. Bathymetric resolution in each panel indicates the spacing of CTD sections for each year.

between layers are negligible in all summer cases (no larger than 6% of the northwestward flux through S1; Figures 2b, 2c, and 2f).

To investigate the vertical structure of the currents, we map current speed into depth coordinates on the common across-depression section (S1; Figure 1) for years 1999, 2001, 2008a, and 2015 (Figure 3; positive is northwestward). In both summer and winter, northwestward flow occurs in the southern part of the domain and southeastward flow occurs farther north. However, the strength of the southeastward flow is greatly enhanced and the northwestward flow transports higher-density water during winter. The surface to mid-depth southeastward flow of MCDW* in winter is compensated by the northwestward flow of DSW at depth, reflecting the transformation of MCDW* to DSW by surface buoyancy fluxes (Figure 3a). In summer, DSW is no longer formed and the 27.83 kg m^{-3} isopycnal deepens. While a weak southeastward flow is present in all summer cases, the northwestward flow dominates. The northwestward current in summer is surface-intensified in 2015 but is relatively barotropic in 2001 and 2008a (Figures 3b–3d). The change in the summer circulation may be a result of the MGT calving in 2010; however, without a detailed analysis of the momentum budget (beyond the scope of this study) we cannot determine whether the calving influenced the vertical structure of the flow.

4. Discussion

4.1. Wind-Driven Summer Circulation

The katabatic southeasterly winds observed in this region [*Williams and Bindoff*, 2003; *Wendler et al.*, 1997; *Lytle et al.*, 2001; *Parish and Walker*, 2006] drive a southwestward Ekman transport toward the Antarctic coast. Convergence of water against the coast creates an offshore pressure gradient that drives a northwestward geostrophic current, the Antarctic Coastal Current, seen in all summer realizations (Figure 2). Surface buoyancy fluxes during summer reduce surface densities through warming and ice melt, increasing surface stratification, but have little direct influence on the circulation, as illustrated by the weak diapycnal fluxes (Figures 2b–2f). We conclude that winds constitute the primary atmospheric forcing in summer.

The shelf-wide summer coastal current is inconsistent with the gyre structure produced by the Adélie region model of *Kusahara et al.* [2011a]. The inconsistency likely results from the MGT being treated as land in the model, meaning no water can enter the region from the southeast.

Numerical simulations suggest that the easterly winds regulate the on-shelf transport of MCDW* [*Spence et al.*, 2014; *Stewart and Thompson*, 2012, 2015]. We find the wind-driven circulation in summer transports little

MCDW* onto the shelf in this location, indicating that wind is not the only mechanism influencing cross-shelf exchange (section 4.2).

4.2. Buoyancy-Driven Winter Circulation

In winter, stronger winds [*Parish and Walker*, 2006] and the influence of drifting sea ice in enhancing momentum transfer [*Martin et al.*, 2014, 2016], likely increase the stress exerted at the sea surface. However, unlike in summer, winter surface buoyancy losses via cooling and brine rejection represent an available potential energy (APE) input. Part of the APE is released through convection on the shelf. The remaining APE is released as the DSW sinks to the abyssal ocean via the Adélie Sill. Over the winter polynya, more than 0.29 ± 0.02 Sv of DSW is formed through diapycnal fluxes (Figure 2a); i.e., nearly two thirds of the DSW exported to the northwest is produced through surface buoyancy losses, highlighting the important influence of buoyancy forcing in driving the off-shelf flow of DSW.

Mass conservation on the shelf necessitates that the buoyancy-driven off-shelf flow be compensated by an on-shelf flow. The southeastward on-shelf transport of MCDW* nearly balances the outflow of DSW (section 3), with the Coriolis force setting the cyclonic sense of the circulation. The on-shelf flow of MCDW* is an order of magnitude larger in winter and opposes the coastal current found in the wind-driven summer circulation. These observations suggest that surface buoyancy fluxes that result in diapycnal fluxes to denser water classes dominate over wind stress in driving the winter circulation.

The winter measurements at the shelf break [*Williams and Bindoff*, 2003] are too coarse to suitably constrain an inverse model, and we do not provide direct observations of DSW and MCDW* crossing the shelf break. Both observational and modeling studies have suggested that the primary outflow of DSW occurs in the Adelie Sill and the inflow of MCDW* occurs at the Sill or west of the Mertz Bank [*Marsland et al.*, 2004; *Williams et al.*, 2008, 2010; *Kusahara et al.*, 2011a; *Cougnon et al.*, 2013], a pattern consistent with our measurements. The shallowness of the Mertz Bank (at ≈200 m depth) and the absence of westward flow of MCDW* across S1 (Figure 2a) is consistent with a "local" source of MCDW*.

Williams and Bindoff [2003] similarly use the 1999 winter CTD measurements, along with ADCP velocity constraints, to derive winter shelf circulation. They find a cyclonic circulation broadly consistent with our inverse model. However, the gyre configuration proposed by *Williams and Bindoff* [2003] involves recirculation of DSW southeastward in the northern part of S1. Our results provide no evidence of such a recirculation (Figure 2a). *Williams and Bindoff* [2003] conserved total mass only, while our model conserves total and layer-wise mass, heat and salt, providing a more constrained solution. Furthermore, surface buoyancy fluxes in *Williams and Bindoff* [2003] were implicitly derived from the inverse model, whereas our model includes prescribed buoyancy fluxes derived from direct observations over the polynya.

The single winter snapshot available does not allow an assessment of variability in transport, diapycnal fluxes, and dense water formation nor the role of buoyancy fluxes in driving shelf circulation at interannual time scales. Given the role of buoyancy in driving the flow in the 1999 winter snapshot, we anticipate that the recently reduced polynya activity following the MGT calving [*Tamura et al.*, 2012; *Dragon et al.*, 2014; *Nihashi and Ohshima*, 2015], has weakened the winter circulation, cross-shelf exchange, and DSW formation postcalving. DSW volumes reduced in summer following the calving of the MGT (Figures 2 and 3) and are consistent with a decline in the formation and outflow of DSW in winter.

Increased cross-shelf exchange mediated by the release of APE under increased surface buoyancy losses occurs in both idealized [*Stewart and Thompson*, 2015] and realistic [*Snow et al.*, 2016] models. Numerical simulations by *Marsland et al.* [2004] also find that the Adélie region cross-shelf exchange depends on polynya strength and, in particular, suggest surface buoyancy loss drives exchange of MCDW*. Such modeling results support the hypothesis that winter circulation and the enhanced cross-shelf exchange is a result of surface buoyancy forcing.

5. Conclusion

An inverse box model is used to investigate the drivers of Antarctic shelf circulation and cross-shelf exchange at a key Antarctic Bottom Water (AABW) formation site. We exploit a time series of observations from the Adélie Land region of East Antarctica to explore the characteristics of the shelf circulation under seasonal and interannual changes in surface forcing. The circulation and cross-shelf exchange are significantly different in summer and winter. During summer, wind stresses drive a northwestward coastal current with only a

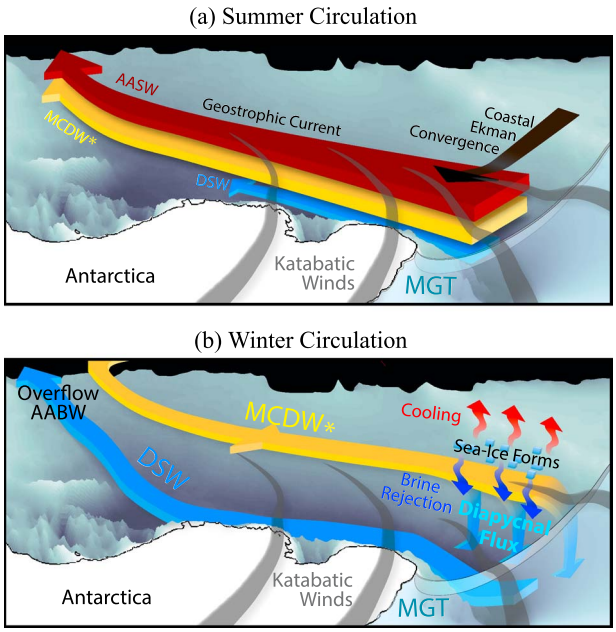

Figure 4. Representation of the (a) summer and (b) winter circulation within the Adélie region, East Antarctica. Red arrows represent AASW, yellow MCDW*, and blue is DSW.

weak on-shelf flow of Modified Circumpolar Deep Water (MCDW*; Figure 4a). The wind-driven coastal current shows no significant changes (that could not be accounted for through interannual variability) in transport subsequent to the Mertz Glacier Tongue (MGT) calving.

During winter, surface buoyancy loss drives a cyclonic circulation and enhanced cross-shelf exchange (Figure 4b). The buoyancy losses form Dense Shelf Water, which flows northwestward off the shelf to sink to the abyssal ocean as AABW. Mass conservation requires a compensating on-shelf flow of MCDW* into the depression. The winter inflow of MCDW* is an order of magnitude larger than in summer consistent with recent modeling studies proposing that buoyancy fluxes influence the cross-shelf exchange [*Stewart and Thompson*, 2015; *Snow et al.*, 2016].

Changes in the cross-shelf exchange of DSW and MCDW* have significant ramifications for ice sheet melt rates [e.g., *Thoma et al.*, 2008; *Dinniman et al.*, 2012], AABW formation, properties and variability [*Snow et al.*, 2016], and the deep meridional overturning circulation [*Stewart and Thompson*, 2012, 2013]. Many characteristics of the Adélie region parallel other key AABW formation areas. By highlighting the significance of surface buoyancy fluxes in controlling the strength of the cross-shelf exchange and circulation, we aid in developing an improved understanding of the drivers of Antarctic shelf circulation, AABW formation processes, and ice-ocean interactions. With the cryospheric and oceanic response to a changing climate integrally connected to changing surface buoyancy fluxes, improved observations of these fluxes is essential for increased understanding of future climate change.

Acknowledgments

B.M.S. and S.R.R. were supported by the Australian Government Department of the Environment and CSIRO through the Australian Climate Change Science Programme. A.M.H. was supported by an Australian Research Council Future Fellowship FT120100842. S.R.R. and S.M.D. were supported by the Australian Government Business Cooperative Research Centres Programme through the Antarctic Climate and Ecosystems Cooperative Research Centre (ACE CRC). The authors would like to thank the captain, crew and scientific party of the RSV Aurora Australis and SV l'Astrolabe for their support in collecting the observational data, with additional thanks to Mark Rosenberg for data processing. The ALBION-2008 voyage was supported by the French LEFE programme and by the Institut Paul Emile Victor (IPEV). Data analyzed in this manuscript are available from the Australian Antarctic Data Centre (https://data.aad.gov.au/).

References

Cougnon, E. A., B. K. Galton-Fenzi, A. J. S. Meijers, and B. Legrésy (2013), Modeling interannual dense shelf water export in the region of the Mertz Glacier Tongue (1992–2007), *J. Geophys. Res. Oceans*, *118*, 5858–5872, doi:10.1002/2013JC008790.

Dinniman, M. S., J. M. Klinck, and E. E. Hofmann (2012), Sensitivity of Circumpolar Deep Water transport and ice shelf basal melt along the West Antarctic Peninsula to changes in the winds, *J. Clim.*, *25*, 4799–4816.

Dragon, A.-C., M.-N. Houssais, C. Herbaut, and J.-B. Charrassin (2014), A note on the intraseasonal variability in an Antarctic polynia: Prior to and after the Mertz Glacier calving, *J. Mar. Syst.*, *130*, 46–55.

Hellmer, H. H., F. Kauker, R. Timmermann, J. Determann, and J. Rae (2012), Twenty-first-century warming of a large Antarctic ice-shelf cavity by redirected coastal currents, *Nature*, *485*, 225–228.

Jacobs, S. S. (2004), Bottom water production and its links with the thermohaline circulation, *Antarct. Sci.*, *4*, 427–4378.

Johnson, G. C. (2008), Quantifying Antarctic bottom water and North Atlantic deep water volumes, *J. Geophys. Res.*, *113*, C05027, doi:10.1029/2007JC004477.

Kuhlbrodt, T., A. Griesel, M. Montoya, A. Levermann, M. Hofmann, and S. Rahmstorf (2007), On the driving processes of the Atlantic meridional overturning circulation, *Rev. Geophys.*, *45*, RG2001, doi:10.1029/2004RG000166.

Kusahara, K., H. Hasumi, and T. Tamura (2010), Modeling sea ice production and dense shelf water formation in coastal polynyas around East Antarctica, *J. Geophys. Res.*, *115*, C10006, doi:10.1029/2010JC006133.

Kusahara, K., H. Hasumi, and G. D. Williams (2011a), Dense shelf water formation and brine-driven circulation in the Adélie and George V Land region, *Ocean Model.*, *37*, 122–138.

Kusahara, K., H. Hasumi, and G. D. Williams (2011b), Impact of the Mertz Glacier Tongue calving on dense water formation and export, *Nat. Commun.*, *37*, 122–138.

Lacarra, M., M.-N. Houssais, E. Sultan, S. R. Rintoul, and C. Herbaut (2011), Summer hydrography on the shelf off Terre Adélie/George V Land based on the ALBION and CEAMARC observations during the IPY, *Polar Sci.*, *5*, 88–103.

Lacarra, M., M.-N. Houssais, C. Herbaut, E. Sultan, and M. Beauverger (2014), Dense shelf water production in the Adélie Depression, East Antarctica, 2004–2012: Impact of the Mertz Glacier calving, *J. Geophys. Res. Oceans*, *119*, 5203–5220, doi:10.1002/2013JC009124.

Lytle, V. I., A. P. Worby, R. Massom, M. J. Paget, I. Allison, X. Wu, and A. Roberts (2001), Ice formation in the Mertz Glacier polynya, East Antarctica, during winter, *Ann. Glaciol.*, *33*, 368–372.

Marsland, S. J., N. L. Bindoff, G. D. Williams, and W. F. Budd (2004), Modeling water mass formation in the Mertz Glacier Polynya and Adélie Depression, East Antarctica, *J. Geophys. Res.*, *109*, C11003, doi:10.1029/2004JC002441.
Martin, T., M. Steele, and J. Zhang (2014), Seasonality and long-term trend of Arctic Ocean surface stress in a model, *J. Geophys. Res. Oceans*, *119*, 1723–1738, doi:10.1002/2013JC009425.
Martin, T., M. Tsamados, and D. Schroeder (2016), The impact of variable sea ice roughness on changes in Arctic Ocean surface stress: A model study, *J. Geophys. Res. Oceans*, *121*, 1931–1952, doi:10.1002/2015JC011186.
McDougall, T. J., and P. M. Barker (2011), Getting started with TEOS-10 and the Gibbs Seawater (GSW) Oceanographic Toolboxs, *Tech. Rep.*, 28 pp., SCOR/IAPSO WG127, ISBN 978-0-646-55621-5.
Nihashi, S., and K. I. Ohshima (2015), Circumpolar mapping of Antarctic coastal polynyas and landfast sea ice: Relationship and variability, *J. Clim.*, *28*, 3650–3670.
Parish, T. R., and R. Walker (2006), A re-examination of the winds of Adélie Land, Antarctica, *Aust. Meteorol. Mag.*, *55*, 105–117.
Purkey, S. G., and G. C. Johnson (2013), Antarctic bottom water warming and freshening: Contributions to sea level rise, ocean freshwater budgets, and global heat gain, *J. Clim.*, *26*, 6105–6122.
Rintoul, S. R. (1998), On the origin and influence of Adélie Land bottom water, in *Ocean, Ice, and Atmosphere: Interactions at the Antarctic Continental Margin*, edited by S. Jacobs and R. Weiss, pp. 151–172, AGU, Washington, D. C.
Ríos, A. F., A. Velo, P. C. Pardo, M. Hoppema, and F. F. Pérez (2012), An update of anthropogenic CO_2 storage rates in the western South Atlantic basin and the role of Antarctic bottom water, *J. Mar. Syst.*, *94*, 197–203.
Roberts, A., A. Allison, and V. I. Lytle (2001), Sensible- and latent-heat-flux estimates over the Mertz Glacier polynya, East Antarctica, from in-flight measurements, *Ann. Glaciol.*, *33*, 377–384.
Rosenberg, M., and S. R. Rintoul (2010), Aurora Australis Marine Science Cruise AU0803 and AU0806—Oceanographic field measurements and analysis, Antarctic Climate & Ecosystems Cooperative Research Centre, Hobart, Australia, 2010 unpublished report.
Rosenberg, M., and S. R. Rintoul (2011), Aurora Australis Marine Science Cruise AU1121—Oceanographic field measurements and analysis, Antarctic Climate & Ecosystems Cooperative Research Centre, Hobart, Australia, 2011 unpublished report.
Rosenberg, M., and S. R. Rintoul (2015), Aurora Australis Marine Science Cruise AU1402—Oceanographic field measurements and analysis, Antarctic Climate & Ecosystems Cooperative Research Centre, Hobart, Australia, 2015 unpublished report.
Rosenberg, M., N. L. Bindoff, S. Bray, C. Curran, I. Helmond, J. Miller, D. McLachlan, and J. Richman (2001), Mertz Polynya Experiment, Marine Science Cruises AU9807, AU9801, AU9905, AU9901 and TA0051—Oceanographic field measurements and analysis, *Antarctic CRC Res. Rep. No. 25*, Antarctic Climate & Ecosystems Cooperative Research Centre, Hobart, Australia.
Sloyan, B. M., and S. R. Rintoul (2000), Estimates of area-averaged diapycnal fluxes from basin-scale budgets, *J. Phys. Oceanogr.*, *30*, 2320–2341.
Sloyan, B. M., and S. R. Rintoul (2001a), The Southern Ocean limb of the global deep overturning circulation, *J. Phys. Oceanogr.*, *31*, 143–173.
Sloyan, B. M., and S. R. Rintoul (2001b), Circulation, renewal, and modification of Antarctic mode and intermediate water, *Geophys. Res. Lett.*, *28*, 2049–2052.
Sloyan, B. M., and J. Schröter (2001), Correlation of ocean mass and temperature fluxes among hydrographic sections in the southern oceans, *J. Phys. Oceanogr.*, *31*, 1005–1030.
Snow, K., A. M. Hogg, B. M. Sloyan, and S. M. Downes (2016), Sensitivity of Antarctic bottom water to changes in surface buoyancy fluxes, *J. Clim.*, *29*, 313–330.
Spence, P., S. M. Griffies, M. H. England, A. M. Hogg, O. A. Saenko, and N. C. Jourdain (2014), Rapid subsurface warming and circulation changes of Antarctic coastal waters by poleward shifting winds, *Geophys. Res. Lett.*, *41*, 4601–4610, doi:10.1002/2014GL060613.
Stewart, A. L., and A. F. Thompson (2012), Sensitivity of the ocean's deep overturning circulation to easterly Antarctic winds, *Geophys. Res. Lett.*, *39*, L18604, doi:10.1029/2012GL053099.
Stewart, A. L., and A. F. Thompson (2013), Connecting Antarctic cross-slope exchange with Southern Ocean overturning, *J. Phys. Oceanogr.*, *43*, 1453–1471.
Stewart, A. L., and A. F. Thompson (2015), Eddy-mediated transport of warm Circumpolar Deep Water across the Antarctic shelf break, *Geophys. Res. Lett.*, *42*, 432–440, doi:10.1002/2014GL062281.
Tamura, T., K. I. Ohshima, and S. Nihashi (2008), Mapping of sea ice production for Antarctic coastal polynyas, *Geophys. Res. Lett.*, *35*, L07606, doi:10.1029/2007GL032903.
Tamura, T., G. D. Williams, A. D. Fraser, and K. I. Ohshima (2012), Potential regime shift in decreased sea ice production after the Mertz Glacier calving, *Nat. Commun.*, *3*, 826.
Thoma, M., A. Jenkins, D. Holland, and S. Jacobs (2008), Modelling Circumpolar Deep Water intrusions on the Amundsen Sea continental shelf, Antarctica, *Geophys. Res. Lett.*, *35*, L18602, doi:10.1029/2008GL034939.
Wendler, G., C. Stearns, G. Weidner, and G. Dargaud (1997), On the extraordinary katabatic winds of Adélie Land, *J. Geophys. Res.*, *102*, 4463–4474.
Williams, G. D., and N. L. Bindoff (2003), Wintertime oceanography of the Adélie Depression, *Deep Sea Res., Part II*, *50*, 1373–1392.
Williams, G. D., N. L. Bindoff, S. J. Marsland, and S. R. Rintoul (2008), Formation and export of dense shelf water from the Adélie Depression, East Antarctica, *J. Geophys. Res.*, *113*, C04039, doi:10.1029/2007JC004346.
Williams, G. D., S. Aoki, S. S. Jacobs, S. R. Rintoul, T. Tamura, and N. L. Bindoff (2010), Antarctic Bottom Water from the Adélie and George V Land coast, East Antarctica (140–149°E), *J. Geophys. Res.*, *115*, C04027, doi:10.1029/2009JC005812.
Wunsch, C. (1978), The North Atlantic general circulation west of 50°W determined by inverse methods, *Rev. Geophys.*, *16*, 583–620.
Wunsch, C. (1996), *The Ocean Circulation Inverse Problem*, Cambridge Univ. Press, New York.